

Adaptive Internal Models in the Optokinetic System

Erin Battle¹ and Mireille E. Broucke¹

Abstract—We present a control-theoretic model of the optokinetic system, an eye movement system for tracking a moving visual surround. The model adheres to the neural circuit in the brain and is based on the application of adaptive internal models to capture the contribution of the cerebellum. The model is validated through simulations, recovering the basic behaviors of the optokinetic system known from experimental studies.

I. INTRODUCTION

There is no doubt control theory has much to contribute to the understanding of the brain [29]. Nevertheless, the preponderance of recent control-theoretic studies focuses at the micro- or meso-scale, namely on individual or groups of neurons; a sample is [6], [15], [37], [38]. The paucity of control-theoretic brain research at the behavioral level is epitomized for us by the widespread belief in neuroscience on the existence of internal models in the brain [52] without reference to the internal model principle [17] to clarify their form and function. See [24] for a thorough discussion of this dichotomy. An opinion is presented in [31], and interesting related results are presented in [45] from a systems biology perspective.

It is believed that internal models reside in the cerebellum, a part of the brain that performs diverse regulatory functions such as motor control. By 1967, the neural circuit of the cerebellum had been completely mapped out. Shortly following, the Marr-Albus theory proposed that the cerebellum is a pattern recognition data processing system [1], [33]. The model was extended to account for dynamic (time dependent) signal processing in [18]. Subsequently, a nonlinear adaptive control method that learns an *inverse model* of the plant was proposed in [21]. A second theory proposes that the cerebellum learns a *forward model* of the plant [40]. Despite important advances, researchers have not been able to achieve a comprehensive model that could, for instance, reproduce all behaviors of the *oculomotor system*. We are exploring *adaptive internal models* [5], [20], [32], [35], [36], [44] as an alternative method to model the cerebellum [7], [8], [9], [19], [22].

Our focus on the oculomotor system is motivated by the fact that it serves as an exemplar among motor control systems. The structure and computations of the cerebellum are identical across all the systems it regulates, differences arising only in the input/output connections to each cerebellar module. The oculomotor system has a very simple plant (the eyeball), is phylogenetically the oldest motor system, and is believed to provide the blueprint for all other motor systems.

In [7], [8] we presented a model of the vestibulo-ocular reflex (VOR), smooth pursuit, and gaze holding eye movement systems, regulated by the floccular complex (FC), by applying an adaptive internal model design in [44]. The present paper focuses on the *optokinetic system*, another eye movement system regulated by the nodulus/uvula (NU). This second module of the cerebellum works in concert with the FC - how it does so raises interesting architectural questions.

Pioneering experimental work in the 1970's on the optokinetic system [14], [41], [49], [50] lead to the discovery of the velocity storage mechanism (VSM), a behavior in which eye velocity is stored while following a constant velocity visual surround, even with intervening *saccades* (a fast reset of eye position) in a behavior called *nystagmus*. A striking feature of the VSM is that it partially meets the requirements of the internal model principle, as if evolution made a first attempt at architecting a neural internal model for this motor system. Despite a comprehensive experimental record exposing all major behaviors of the optokinetic system, to this day, the two most important mathematical models of the optokinetic system [14], [42] do not include the cerebellum. This paper aims to fill this gap.

II. REGULATOR PROBLEM

In this section we first orient the reader to a design approach that inspires our model of the cerebellum. This *regulator design* will be somewhat more general than what is required for the optokinetic system, but it provides us with a context from which to initiate our modeling work. We consider an open-loop system

$$\dot{x} = Ax + Bu + Bd \quad (1a)$$

$$\dot{w} = (F + G\psi)w \quad (1b)$$

$$d = \psi w \quad (1c)$$

$$e = Cx, \quad (1d)$$

where $x \in \mathbb{R}^n$ is the state, $w \in \mathbb{R}^q$ is the exosystem state, $u \in \mathbb{R}$ is the input, $d \in \mathbb{R}$ is a disturbance, and $e \in \mathbb{R}$ is the regulated output. Notice the exosystem (1b) has already been transformed according to the method in [35]. This is a *disturbance rejection problem* in which a disturbance d enters additively in the control input. The control objective is to drive the error e to zero.

We impose the following standard assumptions:

(A1) (A, B) is controllable and (C, A) is observable.

(A2) $S = F + G\psi$ has simple eigenvalues on the imaginary axis in the complex plane.

(A3) $\det \begin{bmatrix} A - \lambda I & B \\ C & 0 \end{bmatrix} \neq 0$ for all $\lambda \in \sigma(S)$.

¹Supported by the Natural Sciences and Engineering Research Council of Canada (NSERC). Electrical and Computer Engineering, University of Toronto, Toronto ON Canada, broucke@control.utoronto.ca.

- (A4) (F, G) is a controllable pair, $F \in \mathbb{R}^{q \times q}$ is Hurwitz, and (ψ, S) is an observable pair.
(A5) Dimension q is interpreted as a known upper bound on the order of the exosystem, while the exosystem parameters $\psi \in \mathbb{R}^{1 \times q}$ are unknown.
(A6) The parameters (A, B, C) are known.
(A7) The measurement is x .

Remark 1: Several assumptions may be relaxed; for instance, we may replace (A1) by (A, B) is stabilizable. Observability of (ψ, S) is no loss of generality since one can trim the exosystem by removing the unobservable modes without affecting the plant. The upper bound q means that the exosystem may be overmodeled. For instance, a third order exosystem can model the sum of a step signal and a sinusoid, but it can also model a step alone by suitable choice of initial conditions. \triangleleft

The controller takes the form

$$u = u_s + u_{im}, \quad (2)$$

where u_s is for closed-loop stability, and u_{im} is to satisfy the internal model principle. For stabilization, let $u_s = Kx$ such that $(A+BK)$ is Hurwitz. To satisfy the internal model principle, consider the *adaptive internal model* based on a minimal order observer proposed in [36] (therein called a disturbance observer) and given by

$$\dot{w}_0 = Fw_0 + (FN - NA)x - NBu \quad (3a)$$

$$\hat{w} = w_0 + Nx \quad (3b)$$

$$u_{im} = -\hat{\psi}\hat{w}, \quad (3c)$$

where N is selected such that $NB = G$, and $\hat{\psi}$ is an estimate of ψ . Then we have

$$\begin{aligned} \dot{\hat{w}} &= Fw_0 + (FN - NA)x - NBu + N(Ax + Bu + Bd) \\ &= F(w_0 + Nx) + Gd \\ &= F\hat{w} + Gd. \end{aligned} \quad (4)$$

Define $\tilde{w} = w - \hat{w}$. Then $\dot{\tilde{w}} = F\tilde{w}$. The *parameter adaptation rule* is

$$\dot{\hat{\psi}} = \gamma(B^T Px)\hat{w}^T, \quad (5)$$

where $\gamma > 0$ is the adaptation rate, and $P \in \mathbb{R}^{n \times n}$ is the symmetric, positive definite solution of the Lyapunov equation $(A+BK)^T P + P(A+BK) = -Q$, with $Q \in \mathbb{R}^{n \times n}$ symmetric and positive definite. Finally, the controller is

$$u = Kx - \hat{\psi}\hat{w}. \quad (6)$$

Define the *parameter estimation error* $\tilde{\psi} := \psi - \hat{\psi}$. To prove correctness of the regulator design, we recall a standard result of adaptive control [43].

Theorem 2: Consider the system

$$\dot{x} = Ax + B(\tilde{\psi}w) \quad (7a)$$

$$\dot{\tilde{\psi}} = -\gamma(B^T Px)w^T, \quad (7b)$$

where $\gamma > 0$, A is Hurwitz, and P is the symmetric, positive definite solution of $A^T P + PA = -Q$, for some symmetric,

positive definite Q . Suppose $w \in \mathcal{L}_\infty$. Then $x, \tilde{\psi} \in \mathcal{L}_\infty$, and $x(t) \rightarrow 0$.

Theorem 3: Consider the system (1) satisfying assumptions (A1)-(A7), and consider the regulator (3), (5), and (6). Suppose $A + BK$ is Hurwitz. Then $\hat{\psi}, \hat{w} \in \mathcal{L}_\infty$, $x(t), e(t) \rightarrow 0$, and $\tilde{\psi}(t)\hat{w}(t) \rightarrow 0$.

Proof: Applying input (6), the closed loop system is

$$\dot{x} = (A + BK)x + B\tilde{\psi}\hat{w} + B\psi\tilde{w} \quad (8a)$$

$$\dot{\tilde{w}} = F\tilde{w} \quad (8b)$$

$$\dot{\tilde{\psi}} = -\gamma(B^T Px)\hat{w}^T. \quad (8c)$$

Since F is Hurwitz, from (8b) we get $\tilde{w}(t) \rightarrow 0$. Inclusion of \tilde{w} in the stability analysis involves a minor extension of the Lyapunov argument in Theorem 2 based on Young's inequality. For parsimony here we consider stability of the reduced system with states $(x, \tilde{\psi})$

$$\dot{x} = (A + BK)x + B\tilde{\psi}\hat{w} \quad (9a)$$

$$\dot{\tilde{\psi}} = -\gamma(B^T Px)\hat{w}^T. \quad (9b)$$

By assumption (A2), $w \in \mathcal{L}_\infty$, and $\tilde{w}(t) \rightarrow 0$, so $\hat{w} \in \mathcal{L}_\infty$. Hence, the reduced system satisfies all the assumptions of Theorem 2. We conclude $x, \tilde{\psi} \in \mathcal{L}_\infty$, $x(t) \rightarrow 0$, and $e(t) \rightarrow 0$. Next, from (9a) we know $\dot{x} \in \mathcal{L}_\infty$; from (9b) we know $\dot{\tilde{\psi}} \in \mathcal{L}_\infty$; and from (4), $\dot{\hat{w}} \in \mathcal{L}_\infty$. Then considering

$$\ddot{x} = (A + BK)\dot{x} + B\dot{\tilde{\psi}}\hat{w} + B\tilde{\psi}\dot{\hat{w}},$$

we deduce that $\ddot{x} \in \mathcal{L}_\infty$, so \dot{x} is uniformly continuous. By Barbalat's Lemma, $\dot{x}(t) \rightarrow 0$. Using (9a), we conclude that $\tilde{\psi}(t)\hat{w}(t) \rightarrow 0$. \blacksquare

One can also use an extended form of the internal model [28], [36]. Suppose the system matrices (A, B) of (1a) take the form $A = \Phi_0 + ae_1^T$, and $B = be_n$, where $\Phi_0 \in \mathbb{R}^{n \times n}$ contains all zeros except for one's on the upper diagonal; e_i is the i th Euclidean coordinate vector; and $a = (a_1, \dots, a_n) \in \mathbb{R}^n$ and $b \in \mathbb{R}$ represent unknown plant parameters. The extended internal model is

$$\dot{w}_0 = Fw_0 + (FN - N\Phi_0)x \quad (10a)$$

$$\dot{w}_1 = Fw_1 - Ne_1^T x_1 \quad (10b)$$

$$\vdots \quad (10c)$$

$$\dot{w}_n = Fw_n - Ne_n^T x_n \quad (10d)$$

$$\dot{w}_{n+1} = Fw_{n+1} - Ne_n u \quad (10e)$$

$$\dot{w} = w_0 + Nx + a_1 w_1 + \dots + a_n w_n + b w_{n+1} \quad (10f)$$

where $w_i \in \mathbb{R}^q$ for $i = 0, \dots, n+1$. We can verify once again that $\dot{w} = F\hat{w} + Gd$, and $\tilde{w} = F\tilde{w}$. While this model does suffer from overparametrization of the unknown parameters ψ , a , and b , its structure is, nevertheless, evocative in our modeling problem (see the comments in the Conclusion).

III. NEURAL CIRCUIT

A model of the optokinetic system would be of limited value if it did not match the neural circuit. We describe its relevant aspects at a high level; see Figure 1.

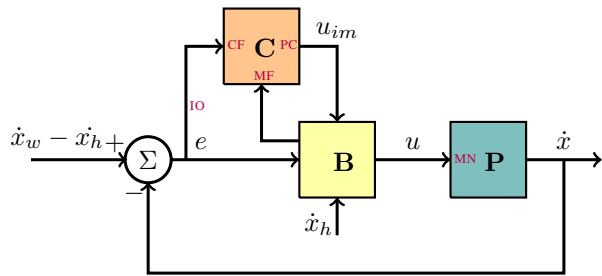


Fig. 1: Control architecture for the optokinetic system consisting of the oculomotor plant (P), the brainstem (B), and the cerebellum (C). The retinal slip velocity e is the error signal to be regulated.

The *visual cortex* processes visual signals arriving from the retina by way of the optic nerve. The *nucleus of the optic tract* (NOT) projects to the *vestibular nuclei* (VN) of the *brainstem* (B). In particular, the NOT sends a measurement of *retinal slip velocity* to the VN [13]. The brainstem comprises several regions (or functions) relevant to the optokinetic system: the VN, the *brainstem neural integrator* (NI), and the *velocity storage mechanism* (VSM). The VN act as hubs for signals to and from the cerebellum (see below). The NI provides an eye position signal [25]. The VSM, also believed to be located in the VN [42], provides “velocity storage” of a constant velocity visual surround - in essence approximating a pure integrator to track constant disturbances. Finally, the VN output is sent to the oculomotor neurons (MN) to stimulate the muscles and control eye movements.

Specific modules of the cerebellum that control eye movement include the *floccular complex* (FC), and the *nodulus/uvula* (NU). While the FC was the focus of our prior work [8], here we are interested in the NU which is known to regulate the optokinetic system [23]. All modules of the cerebellum have two types of inputs: *mossy fiber* (MF) inputs and *climbing fiber* (CF) inputs. MF inputs to the NU include: primary afferents from the vestibular nerve (carrying a head velocity signal) [2]; a signal from the VN; and a signal from the NI. The CF input to the NU comes from the NOT by way of the *inferior olive* (IO) [3]. Finally, the NU projects its sole output via its Purkinke cells (PCs) to the VN [10].

IV. OPTOKINETIC SYSTEM

We develop a model of the optokinetic system for horizontal eye motion, informed by the description of the neural circuit and inspired by the presented regulator design. The optokinetic system includes behaviors such as *nystagmus*, consisting of both fast and slow phases of eye motion, so a suitable model of the oculomotor plant is a second-order model [46]. As discussed, the optokinetic system is also supported by the VSM, which can be modelled as a leaky integrator [14], [41]. To support the optokinetic reflex, the brainstem-only pathway of the motor command must include a feedforward component of the *retinal slip velocity*, given

by

$$e := \dot{x}_w - \dot{x}_h - \dot{x}.$$

Signal $\dot{x}_w \in \mathbb{R}$ is the horizontal angular velocity of the visual field, \dot{x}_h is the horizontal angular velocity of the head, and \dot{x} is the horizontal angular velocity of the eye. A non-zero \dot{x}_w is induced in experiments when a subject is seated inside a rotating optical drum.

Taken together, the open-loop model of the oculomotor plant and brainstem for the optokinetic system is

$$\dot{x}_1 = x_2 \quad (11a)$$

$$\dot{x}_2 = \alpha_2(-x_2 - K_x x_1 + u) \quad (11b)$$

$$\dot{\hat{x}} = -K_x \hat{x} + u \quad (11c)$$

$$\dot{v} = -K_v v + K_v e \quad (11d)$$

$$u_b = \alpha_x \hat{x} - \alpha_{\text{vor}} \dot{x}_h + \alpha_{\text{ok}} e + \alpha_v v. \quad (11e)$$

Equations (11a)-(11b) comprise the second-order model of the oculomotor plant. Equation (11c) is the brainstem neural integrator; see [8]. Equation (11d) is the velocity storage integrator. Signal x_1 is the eye angle; $x_2 = \dot{x}$ is the eye angular velocity; u is the motor command, regarded as an acceleration input; \hat{x} is an estimate of x ; v is the state of the velocity storage integrator; $\alpha_{\text{ok}} e$ models the drive provided by the optokinetic reflex, where α_{ok} is the called the *optokinetic gain*; the *vestibulo-ocular reflex* is modeled by $\alpha_{\text{vor}} \dot{x}_h$, where α_{vor} is the *VOR gain*; and $\alpha_v v$ models the drive provided by the velocity storage integrator. The brainstem-only component of the motor command is u_b .

Next we model the cerebellar contribution to the optokinetic system. Experimental evidence supports the idea that the driving signal of the optokinetic system is the retinal slip velocity [42]. Moreover, this is the error signal that the cerebellum regulates to zero. This choice of error signal partitions the work of the cerebellum so that the NU regulates a velocity error, while the FC regulates a positional error. The *error model* associated with the NU is

$$\dot{e} = -\alpha_2 e - \alpha_2 u + \alpha_2 K_x x_1 + \ddot{x}_w - \ddot{x}_h + \alpha_2 \dot{x}_w - \alpha_2 \dot{x}_h.$$

The motor command is split as

$$u = u_b + u_s + u_{im},$$

where u_s is a component for closed-loop stability, and u_{im} is the output of the NU. This error model is highly stable due to the known large value of $\alpha_2 \simeq 250$, so we assume $u_s = 0$. Substituting u_b in the error model and assuming $\hat{x}(t) \equiv x_1(t)$, we have

$$\begin{aligned} \dot{e} &= -\alpha_2(1 + \alpha_{\text{ok}})e - \alpha_2 u_{im} + \alpha_2 \tilde{K}_x \hat{x} \\ &\quad - \alpha_2(1 - \alpha_{\text{vor}})\dot{x}_h - \alpha_2 \alpha_v v + \alpha_2 d, \end{aligned} \quad (12)$$

where $d := \frac{1}{\alpha_2}[\ddot{x}_w - \ddot{x}_h] + \dot{x}_w$ is the disturbance that must be rejected. This model may be regarded as a first-order model of velocity error dynamics, despite the fact that it includes a positional term $\alpha_2 \tilde{K}_x \hat{x}$ arising from an incomplete cancellation of the drift term $K_x x_1$ of the oculomotor plant by the neural integrator (11c). Because the eye position is

constantly reset during nystagmus, x_1 remains small. We therefore treat the positional term as a bounded disturbance acting on the velocity error dynamics. We assume this extra disturbance is not rejected by the cerebellum, so some small steady-state errors will remain.

Experimental evidence supports the idea that the NU is dedicated to constant velocity disturbances [23]; whereas the floccular complex (FC) handles sinusoidal disturbances. Thus, we assume the exosystem associated with the NU is first order. For the internal model we use a modification of the extended design in Section II

$$\dot{w}_0 = Fw_0 + FGe \quad (13a)$$

$$\dot{w}_1 = Fw_1 - Ge \quad (13b)$$

$$\dot{w}_2 = Fw_2 - Gu_{im} \quad (13c)$$

$$\dot{w}_3 = Fw_3 - G\hat{x} \quad (13d)$$

$$\dot{w}_4 = Fw_4 - G\hat{x}_h \quad (13e)$$

$$\dot{w}_5 = Fw_5 - Gv \quad (13f)$$

$$\begin{aligned} \hat{w} = & \frac{1}{\alpha_2}w_0 + \frac{1}{\alpha_2}Ge - (1 + \alpha_{ok})w_1 - w_2 \quad (14) \\ & + \tilde{K}_x w_3 - (1 - \alpha_{vor})w_4 - \alpha_v w_5. \end{aligned}$$

What distinguishes this model from a standard regulator design is the appearance of feedforward signals \hat{x} , \hat{x}_h , and v whose inclusion is predicated by the neural circuit; thus the additional filters (13d)-(13f).

Taking the derivative of \hat{w} and utilizing (12), we verify $\dot{\hat{w}} = F\hat{w} + Gd$. If the plant parameters were known, then \hat{w} would provide a regressor for parameter adaptation. Since these parameters are not known, we used the extended regressor and parameters $\psi_d^T := \left(\frac{1}{\alpha_2}\psi, -(1 + \alpha_{ok})\psi, -\psi, \tilde{K}_x\psi, -(1 - \alpha_{vor})\psi, -\alpha_v\psi\right)$ and $\hat{w}_d := (w_0 + Ge, w_1, w_2, w_3, w_4, w_5)$. Then $d = \psi w = \psi\hat{w} + \varepsilon = \psi_d\hat{w}_d + \varepsilon$, where $\varepsilon = \psi\tilde{w}$ vanishes exponentially. Finally, we choose

$$u_{im} = \hat{\psi}_d\hat{w}_d, \quad (15)$$

where $\hat{\psi}_d$ is an estimate of the unknown parameters ψ_d . The parameter adaptation rule is

$$\dot{\hat{\psi}}_d = \gamma e\hat{w}_d^T, \quad (16)$$

where $\gamma > 0$ is the adaptation rate.

Remark 4: A mapping between the neural circuit and signals in our model is the following. Referring to (11e), the output of the neural integrator is the signal $\alpha_v\hat{x}$; the direct feedthrough of the retinal slip velocity to support the optokinetic reflex is the signal $\alpha_{ok}e$; and the output of the VSM is $\alpha_v v$. Signal e in (16) is the projection from the IO to the CF input of the cerebellum. Signals e , u_{im} , \hat{x} , \hat{x}_h , and v in (13) are the MF inputs to the cerebellum. The PC output of the cerebellum is u_{im} . \triangleleft

V. STABILITY ANALYSIS

Our stability analysis focuses on the case when there is no head movement, $\dot{x}_h = 0$. Also, we only study the envelope

behavior of the eye velocity (see Figure 2) by ignoring the velocity resets caused by saccades. This assumption is reasonable due to the very fast initial rise of velocity in the slow phase of nystagmus following a saccade due to the optokinetic reflex. A full hybrid stability analysis is of interest theoretically, though it may not add significantly to the plausibility of the model from a neuroscience perspective.

We begin with a nominal case when $\tilde{K}_x = 0$, meaning there is no perturbation due to eye position. Define the parameter estimation error $\tilde{\psi}_d = \psi_d - \hat{\psi}_d$. Then the closed-loop system is

$$\dot{e} = -\alpha_2(1 + \alpha_{ok})e - \alpha_2\alpha_v v + \alpha_2\tilde{\psi}_d\hat{w}_d \quad (17a)$$

$$\dot{v} = -K_v v + K_v e \quad (17b)$$

$$\dot{\tilde{\psi}}_d = -\gamma e\hat{w}_d^T. \quad (17c)$$

Notice we omitted the exponentially stable \tilde{w} dynamics (see the justification in the proof of Theorem 3). Define the state $\xi := (e, v) \in \mathbb{R}^2$. Then we can write (17) as

$$\dot{\xi} = A\xi + B\tilde{\psi}_d\hat{w}_d \quad (18a)$$

$$e = C\xi \quad (18b)$$

$$\dot{\tilde{\psi}}_d = -\gamma e\hat{w}_d^T, \quad (18c)$$

where

$$A = \begin{bmatrix} -\alpha_2(1 + \alpha_{ok}) & -\alpha_2\alpha_v \\ K_v & -K_v \end{bmatrix}, B = \begin{bmatrix} \alpha_2 \\ 0 \end{bmatrix}, C = [1 \quad 0].$$

Recall that a strictly proper rational $H(s)$ is *strictly positive real* (SPR) if there exists $\epsilon > 0$ such that $\Re[H(s - \epsilon)] \geq 0$, for all $s \in \mathbb{C}$ with $\Re(s) \geq 0$.

Lemma 5: A transfer function $H(s)$ is SPR if and only if $H(s)$ is stable and $\Re[H(j\omega)] > 0, \forall \omega \geq 0$.

Lemma 6: Consider the error model (18) with $\alpha_2, \alpha_{ok}, \alpha_v, K_v > 0$. Then $H(s) = C(sI - A)^{-1}B$ is SPR.

Proof: According to Lemma 5, we must first verify A is Hurwitz. The characteristic polynomial is $\det(sI - A) = s^2 + (K_v + \alpha_2(1 + \alpha_{ok}))s + \alpha_2K_v(1 + \alpha_{ok} + \alpha_v)$. Since the coefficients are strictly positive, A is Hurwitz. Second, we compute $H(j\omega) =$

$$\frac{\alpha_2(j\omega + K_v)}{(\alpha_2K_v(1 + \alpha_{ok} + \alpha_v) - \omega^2) + j\omega(K_v + \alpha_2(1 + \alpha_{ok}))}.$$

Then we have $\Re[H(j\omega)] =$

$$\frac{\alpha_2^2 K_v^2 (1 + \alpha_{ok} + \alpha_v) + \alpha_2^2 \omega^2 (1 + \alpha_{ok})}{(\alpha_2 K_v (1 + \alpha_{ok} + \alpha_v) - \omega^2)^2 + \omega^2 (K_v + \alpha_2 (1 + \alpha_{ok}))^2} > 0,$$

where we use $\alpha_2, \alpha_{ok}, \alpha_v, K_v > 0$, by assumption. By Lemma 5, $H(s)$ is SPR. \blacksquare

The main findings from adaptive control for the considered error model are the following. Recall that $w : \mathbb{R}^+ \rightarrow \mathbb{R}^q$ is *persistently exciting* (PE) if there exist $c_1, c_2, \delta > 0$ such that $c_1 I \leq \int_{t_0}^{t_0 + \delta} w(\tau)w(\tau)^T d\tau \leq c_2 I$, for all $t_0 \geq 0$.

Theorem 7 ([43]): Consider (18). Suppose that $H(s) = C(sI - A)^{-1}B$ is SPR. Then $\xi, e, \tilde{\psi}_d \in \mathcal{L}_\infty$.

(i) If $\hat{w}_d \in \mathcal{L}_\infty$, then $e(t) \rightarrow 0$.

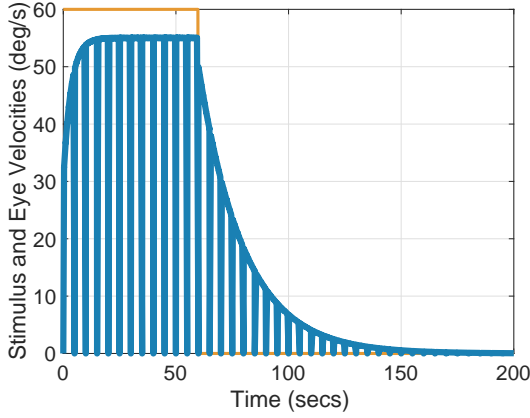


Fig. 2: Untrained OKN and OKAN I

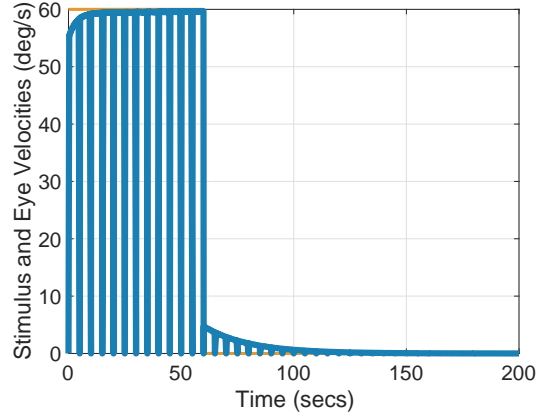


Fig. 3: Trained OKN and OKAN I

- (ii) If $\hat{w}_d, \dot{\hat{w}}_d \in \mathcal{L}_\infty$ and \hat{w}_d is PE, then the equilibrium $(\xi, \tilde{\psi}_d^T) = (0, 0)$ of (18) is globally exponentially stable. We apply this result to our model.

Theorem 8: Consider (18) with $\alpha_2, \alpha_{ok}, \alpha_v, K_v > 0$. Suppose $d \neq 0$ is a constant disturbance. Then the equilibrium $(\xi, \tilde{\psi}_d) = (0, 0)$ is globally exponentially stable.

Proof: By Lemma 6, $H(s)$ is SPR. Since d is a non-zero constant disturbance, w is also constant and non-zero, so it and \hat{w}_d are PE. Also, $\hat{w}_d, \dot{\hat{w}}_d \in \mathcal{L}_\infty$. By Theorem 7, the equilibrium $(\xi, \tilde{\psi}_d) = (0, 0)$ is globally exponentially stable. ■

Now we consider the case when $\tilde{K}_x \neq 0$. Now the closed-loop system is

$$\dot{\xi} = A\xi + B\tilde{\psi}_d\hat{w}_d + B\nu \quad (19a)$$

$$e = C\xi \quad (19b)$$

$$\dot{\tilde{\psi}}_d = -\gamma e \hat{w}_d^T, \quad (19c)$$

where $\nu := \tilde{K}_x \hat{x}$ is regarded as a bounded, unmodeled disturbance. Recall (19) is said to be *input-to-state stable* (ISS) if there exists a class \mathcal{KL} function $\beta_1(\cdot)$ and a class \mathcal{K} function $\beta_2(\cdot)$ such that for any $(\xi(0), \psi_d(0))$ and any $\nu \in \mathcal{L}_\infty$, $\|\xi(t)\| \leq \beta_1(\|\xi(0)\|, t) + \beta_2(\sup_{0 \leq \tau \leq t} \|\nu(\tau)\|)$.

Theorem 9: Consider the closed-loop system (19) with $\alpha_2, \alpha_{ok}, \alpha_v, K_v > 0$. Suppose $d \neq 0$ is a constant disturbance. Then (19) is ISS.

Proof: The result follows by applying Lemma 4.6 of [26]. ■

VI. SIMULATIONS

We examine five basic behaviors of the optokinetic system. The parameter values for the simulations are: $\alpha_2 = 250$, $K_x = 5$, $K_v = 0.05$, $\alpha_v = 10$, $\alpha_{ok} = 1$, $\alpha_{vor} = 0.65$, $\alpha_x = K_x$, $F = -0.01$, $G = 0.01$, and $\gamma = 1e-12$. The parameters α_2 , K_x , and K_v were selected according to the known time constants of the oculomotor plant and the VSM. Parameters $\alpha_v = 10$, $\alpha_{ok} = 1$, and $\alpha_{vor} = 0.65$ are all highly adaptable (through a process of long-term adaptation) and can be selected fairly arbitrarily. The choice $\alpha_x = K_x$ implies that eye position is not a disturbance in these simulations (this is not a requirement however). Parameters F and G

were selected to give a reasonable time constant for the NU. The choice of γ reflects the relatively longer time (on the order of, say, 30 minutes) for the NU to go from trained to untrained conditions. Finally, in order to make the figures easier to view, we display saccades only every 5s. In reality they typically occur roughly every 0.5s [12].

OKN and OKAN I. *Optokinetic nystagmus* (OKN) is perhaps the signature behavior of the optokinetic system. It is an eye movement in which the eye tracks the velocity of a (full-field) moving visual surround during the so-called *slow phase*, followed by a saccade to rapidly reset the eye position to zero in the *fast phase*. OKN is characterized by a fast initial rise in slow-phase eye velocity, followed by a slower rise to a steady-state velocity that nearly matches the velocity of the surround [14, Fig. 3A], [41, Fig. 3B, 4B].

The second signature behavior of the optokinetic system is *optokinetic after-nystagmus I* (OKAN I), a behavior following OKN when the lights are turned off. During OKAN I nystagmus continues in the same direction as OKN, even though there is no visual stimulation. After a quick initial drop, the slow-phase velocity slowly decays to zero during OKAN I [14, Fig 2], [12, Fig 1]; also [41], [48].

Figure 2 shows simulation results for OKN and OKAN I using our model, with the optokinetic drum rotating at a constant velocity of 60 deg/s for 60s. The initial condition on all states and parameters is zero. At the start of OKN, the slow-phase velocity jumps to about 55% of the steady-state value, then rises more slowly and stabilizes around 55°/s. These characteristics can be attributed to the large retinal slip velocity at the onset of the experiment and the charging of the VSM, respectively. The non-zero steady-state error during OKN is observed because the NU internal model is “untrained”, meaning this is the first time the experiment is run with a specific subject.

Once the lights are extinguished at $t = 60$ s, visual signals are no longer present and the cerebellum is effectively inactive, so the signal e is unavailable and $u_{im} = 0$. This causes the slow-phase eye velocity to rely on the dynamics from the VSM, which slowly dissipates its stored velocity, creating OKAN I. The slow-phase velocity experiences a 10% drop, then decays with a time constant of about 18s.

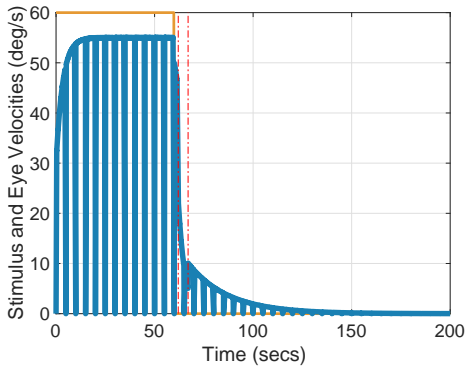


Fig. 4: OKAN suppression with a 5s interval of gaze fixation.

If the subject is involved in repeated trials of the same experiment eliciting OKN and OKAN I, the NU is “trained” over time. In this case, the OKN steady-state slow-phase eye velocity increases [34, Fig 1], the OKAN I time constant decreases [14, Fig 7], and the OKAN I duration decreases [50, Fig 2, 3]. These results are shown in Figure 3, in which all initial conditions are set to zero except the initial condition for $\hat{\psi}_d$, which is set to its true value ψ_d .

OKAN Suppression. *OKAN suppression* or fixation suppression is an experiment in which the lights are turned on for a brief period of time during OKAN, revealing a stationary optokinetic drum on which the subject fixates. Figure 4 shows the results of our model when the lights are turned on 2s after the onset of OKAN I. The lights are left on for 5s, then turned off again. During fixation, the slow-phase eye velocity drops rapidly, as shown between the dashed red lines. This is due to the reappearance of the visual signal e (with $\dot{x}_w = 0$), so the large error causes the velocity signal to drop, along with the inhibitory effects of the cerebellum causing the effective VSM time constant to drop [48]. Once the lights are turned off again, the velocity is able to recover at a depressed value due to the VSM having not dissipated all of its stored activity. Longer fixation periods are known to inhibit the slow-phase velocity so that it cannot recover when the lights are turned off again [14, Fig 8]. For example, with a fixation period of 15s introduced 2s after the onset of OKAN I, the slow-phase eye velocity is completely inhibited, as is shown in Figure 5.

OKN Suppression. *OKN suppression* is an experiment in which a subject fixates on a target straight ahead while the illuminated optokinetic drum is rotating. Although nystagmus is not elicited, the VSM still charges while the drum is moving due to a reduced measurement of e . This causes a small velocity jump at the start of OKAN I when the lights are turned off, followed by a decay to zero [51, Fig 8]. This behaviour is replicated by our model as seen in Figure 6, where we have taken e to be 20% of its full value. We observe that the stored activity of the VSM causes the slow-phase velocity to rise just past $10^\circ/s$ once the lights turn off, to elicit OKAN I.

OKAN II. OKAN II is a second phase of OKAN that arises only after a subject has become habituated to unidirectional

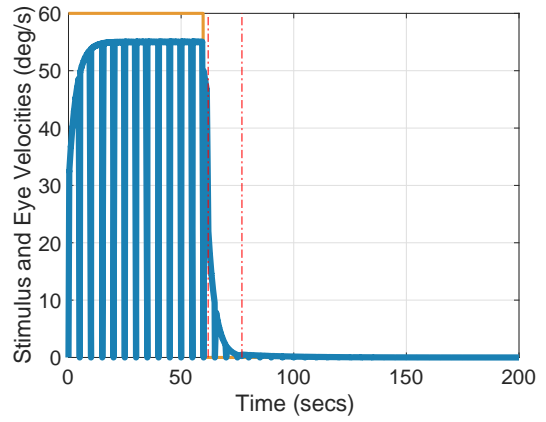


Fig. 5: OKAN suppression with a 15s interval of gaze fixation.

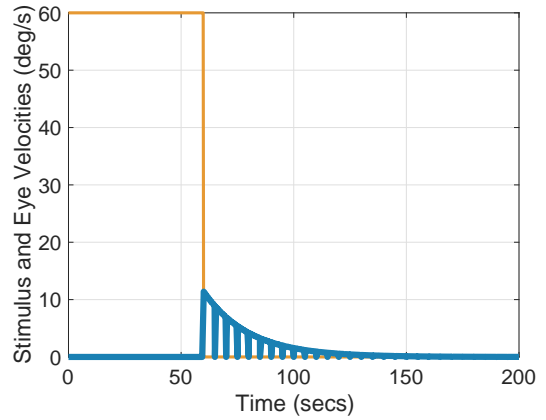


Fig. 6: OKN suppression.

optokinetic stimulation. That is, the optokinetic drum only spins in the positive or negative sense. The presence of OKAN II depends on the duration of the optokinetic stimulation. After potentially many hours of stimulation (lasting 24 hours to 8 days in some experiments [39]), it is observed that the eye velocity in the slow phase of nystagmus reverses direction from the original stimulus direction [50]. OKAN II is believed to arise from a process of long-term adaptation [30], [39], [50] as a compensatory behavior to offset a natural condition called *gaze-evoked nystagmus* in which weakening of the muscles of the eye on one side causes the eye to slip in one direction only, resulting in repeated corrective saccades to maintain steady gaze.

OKAN II may be explained in our model by considering that weakening of the eye muscles in one direction would correspond to a reduction in the parameter K_x for stimulus in the positive sense. We posit that the long-term adaptation process that is activated by prolonged unidirectional nystagmus is a process that calibrates the time constant of the neural integrator via a parameter \hat{K}_x to match the time constant of the oculomotor plant determined by K_x . Instead of utilizing (11c) in which time constants are matched, to elicit OKAN

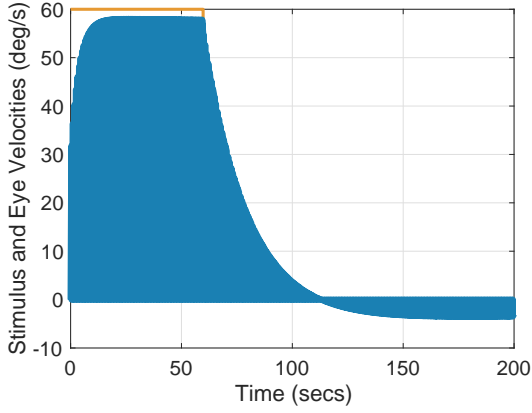


Fig. 7: OKN followed by OKAN I and OKAN II

If we utilize the neural integrator model

$$\dot{\hat{x}} = -\hat{K}_x \hat{x} + u. \quad (20)$$

To model that the muscles have been weakened, we assume $\hat{K}_x \ll K_x$. Define the parameter mismatch

$$\Delta K_x := K_x - \hat{K}_x > 0.$$

Also define the estimation error $\tilde{x} = x - \hat{x}$. Based on a first-order model of the oculomotor plant, a reasonable approximation of the estimation error dynamics is:

$$\dot{\tilde{x}} = -\hat{K}_x \tilde{x} - \Delta K_x x_1.$$

If the optokinetic experiment involves a slow phase on the positive sense, then $x_1(t) \geq 0$ (or on average $x_1(t)$ is positive). Since $\Delta K_x > 0$, $\tilde{x}(t)$ will progressively drift with more negative values.

The oculomotor plant model during OKAN when the lights are off is

$$\begin{aligned} \dot{x}_1 &= x_2 \\ \dot{x}_2 &= \alpha_2(-x_2 - K_x x_1 + \alpha_x \hat{x} + \alpha_v v) \\ &= \alpha_2(-x_2 - \tilde{K}_x x_1 - \alpha_x \tilde{x} + \alpha_v v). \end{aligned}$$

We see that the effect of the mismatch between plant and neural integrator is to introduce a term $\alpha_x \tilde{x}$. The neural integrator generally works to cancel the eye position term $-K_x x_1$ via its contribution $\alpha_x \hat{x}$. Since we now have a parameter mismatch in which $\tilde{K}_x \ll K_x$, we would expect α_x to be greatly reduced as well. We posit that $\alpha_x < 0$ so that the residual signal causes the slow-phase velocity to drift in the negative sense. In summary, OKAN II arises during OKAN when the cerebellum is inactive and when the VSM has depleted its contribution, so $\alpha_v v \simeq 0$. What remains is the negative drive supplied by the drift term $\alpha_x \tilde{x}$.

Our model generates OKAN II with parameter values of $K_x = 5$, $\hat{K}_x = 0.001$, $\alpha_x = -0.002K_x$. Because the results are now dependent on the eye position, the simulations use a small saccade interval to demonstrate more realistic values. Figure 7 shows an experiment starting with 60s of unidirectional optokinetic stimulation before the lights are extinguished. OKAN I proceeds for about 53s as it decays

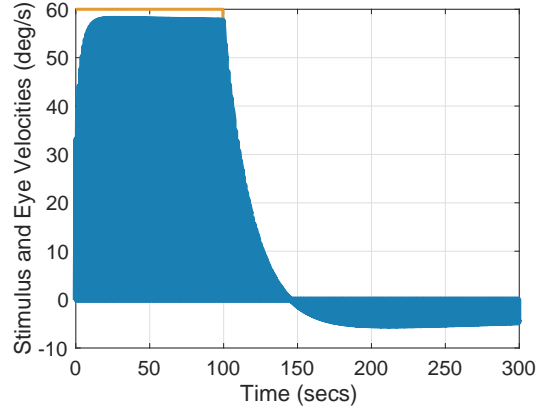


Fig. 8: Longer duration of OKN, followed by OKAN I and OKAN II

to zero. Now the appearance of OKAN II is observed as the slow-phase velocity switches to being negative due to the negative positional term $\alpha_x \tilde{x}$. The velocity peaks at about $-3.5^\circ/s$, and eventually decays to zero (not pictured). These characteristics are comparable to behavioral studies [12, Fig 1].

With repeated trials or a longer stimulus duration, OKAN I is known to decrease in duration while OKAN II is known to increase in peak velocity and in duration [50, Fig 2], [12, Fig 2]. Figure 8 shows results with our model over 100s of optokinetic stimulation in the positive sense. Comparing to Figure 7, the duration of OKAN I has decreased and the peak velocity of OKAN II has indeed increased with a longer stimulation duration.

VII. CONCLUSION

We presented a model of the optokinetic system that includes the computations of the cerebellum and recovers five standard behaviors of this eye movement system. The model is inspired by our hypothesis that the primary function of the cerebellum is disturbance rejection. An architectural feature of the model is the use of feedforward signals from sensory inputs; for instance (13e) utilizes a head velocity signal from the semicircular canals of the ears. Such feedforward signals may provide a mechanism by which parallel internal models work together. Further investigation is needed on this interesting question (indeed we did not include head movement in the present simulation study).

We did not simulate the passage from an untrained to trained NU since, in practice, the simulation time would be too long. On the other hand, making γ larger for faster parameter convergence results in unrealistic transients. The main issue appears to be that the NU model (13), while consistent with the neural circuit, is overparameterized. This phenomenon of poor transients with faster parameter adaptation need not a priori imply a modeling error, as parameter adaptation (depending on the species) appears to occur slowly in the brain. It does echo known limitations on transient performance in adaptive control. Continued theoretical development of adaptive internal models is a

crucial area for future work by control theorists to address such limitations.

REFERENCES

- [1] J. Albus. A theory of cerebellar function. *Mathematical Biosciences*. No. 10, pp. 25–61, 1971.
- [2] N. Barmack, R. Baughman, P. Errico, and H. Shojaku. Vestibular primary afferent projection to the cerebellum of the rabbit. *J. Comp. Neurol.* Vol. 327, pp. 521–534, 1993.
- [3] N. Barmack. Inferior olive and oculomotor system. *Progress in Brain Research*. No. 151, pp. 269–291, 2006.
- [4] N. Barmack and B. Nelson. Influence of long-term optokinetic stimulation on eye movements of the rabbit. 1987.
- [5] H. Basturk and M. Krstic. Adaptive cancellation of matched unknown sinusoidal disturbances for LTI systems by state derivative feedback. *J. Dynamic Systems, Measurement, and Control*. Vol. 135, January 2013.
- [6] F. Blanchini, H. El-Samad, G. Giorano, and E. Sontag. Control-theoretic methods for biological networks. *IEEE Conf. Decision and Control*. December 2018.
- [7] M.E. Broucke. Model of the oculomotor system based on adaptive internal models. *IFAC World Congress*. July 2020.
- [8] M.E. Broucke. Adaptive internal model theory of the oculomotor system and the cerebellum. *IEEE Trans. Automatic Control*. February 2021.
- [9] M.E. Broucke. On the use of regulator theory in neuroscience with implications for robotics. *18th International Conference on Informatics in Control, Automation, and Robotics*. July 2021.
- [10] U. Büttner and J. Büttner-Ennever. Present concepts of oculomotor organization. *Prog. Brain Research*. Vol. 151, pp. 1–42, 2006.
- [11] U. Büttner and W. Waespe. Purkinje cell activity in the primate flocculus during optokinetic stimulation, smooth pursuit eye movements, and VOR-suppression. *Exp. Brain Res.* No. 55, pp. 97–104, 1984.
- [12] U. Büttner, W. Waespe, and V. Henn. Duration and direction of optokinetic after-nystagmus as a function of stimulus exposure time in the monkey. *Arch. Psychiat. Nervenkr.* Vol. 222, pp. 281–291, 1976.
- [13] J. Büttner-Ennever and A. Horn. Anatomical substrates of oculomotor control. *Current Opinion in Neurobiology*. Vol. 7, pp. 872–879, 1997.
- [14] B. Cohen, V. Matsuo, and T. Raphan. Quantitative analysis of the velocity characteristics of optokinetic nystagmus and optokinetic after-nystagmus. *J. Physiology*. Vol. 270, pp. 321–344, 1977.
- [15] G. Drion, A. Franci, and R. Sepulchre. Cellular switches orchestrate rhythmic circuits. *Biol. Cybern.* No. 113, pp. 71–82, 2019.
- [16] J. Eccles, M. Ito, and J. Szentagothai. *The Cerebellum as a Neuronal Machine*. Springer-Verlag, 1967.
- [17] B.A. Francis and W.M. Wonham. The internal model principle of control theory. *Automatica*. Vol. 12, pp. 457–465, 1976.
- [18] M. Fujita. Adaptive filter model of the cerebellum. *Biol. Cybern.* Vol. 45, pp. 195–206, 1982.
- [19] A. Gawad and M.E. Broucke. Visuomotor adaptation is a disturbance rejection problem. *IEEE Conf. Decision and Control*. December 2020.
- [20] D. Gerasimov, A. Miliushin, and V. Nikiforov. Algorithms for adaptive tracking of unknown multisinusoidal signals in linear systems with arbitrary input delay. *Int. J. Adapt. Control Signal Process.* pp. 1–13, 2019.
- [21] M. Kawato and H. Gomi. A computational model of four regions of the cerebellum based on feedback-error learning. *Biol. Cybern.* Vol. 68, pp. 95–103, 1992.
- [22] M. Hafez, E. Uzeda, and M.E. Broucke. Discrete-time output regulation and visuomotor adaptation. *IEEE Conf. Decision and Control*. December 2021.
- [23] S. Heinen and E. Keller. The function of the cerebellar uvula in monkey during optokinetic and pursuit eye movements: single-unit responses and lesion effects. *Exp Brain Research*. Vol. 110, pp. 1–14, 1996.
- [24] J. Huang, A. Isidori, L. Marconi, M. Mischiati, E. Sontag, and W.M. Wonham. Internal models in control, biology, and neuroscience. *IEEE Conf. Decision and Control*. December 2018.
- [25] C. Kaneko. Eye movement deficits after ibotenic acid lesions of the nucleus prepositus hypoglossi in monkeys. ii. pursuit, vestibular, and optokinetic. *J. Neurophysiol* No. 81, pp. 668–681, 1999.
- [26] H. Khalil. *Nonlinear Systems*. 3rd Ed. Pearson, 2001.
- [27] R. Krauzlis, M. Basso, and R. Wurtz. Shared motor error for multiple eye movements. *Science*. No. 276, pp. 1693–1695, 1997.
- [28] M. Krstic, I. Kanellakopoulos, and P. Kokotovic. *Nonlinear and Adaptive Control Design*. Wiley-Interscience, 1995.
- [29] M. Madhav and N. Cowan. The synergy between neuroscience and control theory: the nervous system as inspiration for hard control challenges. *Annu. Rev. Control Robot. Auton. Syst.* No. 3, pp. 243–267, 2020.
- [30] C. Maioli. Optokinetic nystagmus: modeling the velocity storage mechanism. *J. Neuroscience*. No. 8, pp. 821–832, 1988.
- [31] M. Manto and A. Shaikh. Editorial: predictive mechanisms of the cerebello-cerebral networks. *Frontiers in Cellular Neuroscience*. December 2019.
- [32] R. Marino and P. Tomei. An adaptive learning regulator for uncertain minimum phase systems with undermodeled unknown exosystems. *Automatica*. No. 47, pp. 739–747, 2011.
- [33] D. Marr. A theory of the cerebellar cortex. *Journal of Physiology*. No. 202, pp. 437–470, 1969.
- [34] S. Miki, K. Urase, R. Baker, and Y. Hirata. Velocity storage mechanism drives a cerebellar clock for predictive eye velocity control. *Scientific Reports*. Vol. 10, pp. 1–13, 2020.
- [35] V. O. Nikiforov. Adaptive servocompensation of input disturbances. *IFAC World Congress*. pp. 5114–5119, 1996.
- [36] V. O. Nikiforov. Observers of external deterministic disturbances II. Objects with unknown parameters. *Automation and Remote Control*. Vol. 65, No. 11, pp. 1724–1732, 2004.
- [37] E. Nozari and J. Cortes. Hierarchical selective recruitment in linear-threshold brain networks: Parts I & II. *IEEE Trans. Auto. Control*. Vol. 66, Issue 3, pp. 949–980, March 2021.
- [38] N. Olsman, F. Xiao, and J. Doyle. Architectural principles for characterizing the performance of antithetic integral feedback networks. *iScience*. Vol. 14, pp. 277–291, April 2019.
- [39] V. Pettorossi, P. Errico, A. Ferraresi, and N. Barmack. Optokinetic and vestibular stimulation determines the spatial orientation of negative optokinetic after-nystagmus in the rabbit. *J. Neuroscience*. Vol. 19, No. 4, pp. 1524–1531, 1999.
- [40] J. Porrill, P. Dean, and J. Stone. Recurrent cerebellar architecture solves the motor-error problem. *Proc. Royal Soc. Lond. B*. No. 271, pp. 789–796, 2004.
- [41] T. Raphan, V. Matsuo, and B. Cohen. Velocity storage in the vestibulo-ocular reflex arc (VOR). *Experimental Brain Research*. Vol. 35, pp. 229–248, 1979.
- [42] D.A. Robinson. The use of control systems analysis in the neurophysiology of eye movements. *Ann. Rev. Neuroscience*. No. 4, pp. 463–503, 1981.
- [43] S. Sastry and M. Bodson. *Adaptive Control: Stability, Convergence, and Robustness*. Prentice Hall, 1989.
- [44] A. Serrani, A. Isidori, L. Marconi. Semiglobal nonlinear output regulation with adaptive internal model. *IEEE Transactions on Automatic Control*. Vol. 46, No. 8, pp. 1178–1194, 2001.
- [45] E. D. Sontag. Adaptation and regulation with signal detection implies internal model. *Systems Control Lett.* No. 2, Vol. 50, pp. 119–126, 2003.
- [46] P. Sylvestre and K. E. Cullen. Quantitative analysis of abducens neuron discharge dynamics during saccadic and slow eye movements. *Journal of Neurophysiology*. Vol. 82, issue 5, pp. 2612–2632, November 1999.
- [47] W. Waespe, B. Cohen, and T. Raphan. Role of the flocculus and paraflocculus in optokinetic nystagmus and visual-vestibular interactions: effect of lesions. *Experimental Brain Research*. Vol. 50, pp. 9–33, 1983.
- [48] W. Waespe, B. Cohen, and T. Raphan. Dynamic modification of the vestibulo-ocular reflex by the nodulus and uvula. *Science*. Vol. 228, pp. 199–202, 1984.
- [49] W. Waespe and V. Henn. Conflicting visual-vestibular stimulation and vestibular nucleus activity in alert monkeys. *Experimental Brain Research*. Vol. 33, pp. 203–211, 1978.
- [50] W. Waespe and V. Henn. Reciprocal changes in primary and secondary optokinetic after-nystagmus (OKAN) produced by repetitive optokinetic stimulation in the monkey. *Arch. Psychiat. Nervenkr.* Vol. 225, pp. 23–50, 1978.
- [51] W. Waespe and U. Schwarz. Characteristics of eye velocity storage during periods of suppression and reversal of eye velocity in monkeys. *Experimental Brain Research*. Vol. 65, pp. 49–58, 1986.
- [52] D. Wolpert, R.C. Miall, and M. Kawato. Internal models in the cerebellum. *Trends in Cognitive Sciences*. Vol. 2, no. 9, pp. 338–347, September 1998.